Proc. of the 8th International Symposium on Geotechnical Safety and Risk (ISGSR)
Edited by Jinsong Huang, D.V. Griffiths, Shui-Hua Jiang, Anna Giacomini and Richard Kelly
 Published by Research Publishing, Singapore.
doi: 10.3850/978-981-18-5182-7_14-002-cd

ISGSR 2022

Probabilistic Assessment of Spatial Distribution of Soil Liquefaction Potential Using Cone Penetration Test

ZhengGuan[1] and Yu Wang[2]

[1]State Key Laboratory of Internet of Things for Smart City, Department of Civil and Environmental Engineering, University of Macau, Macao, China.
E-mail: guanzheng@um.edu.mo
[2]Department of Architecture and Civil Engineering, City University of Hong Kong, Tat Chee Avenue, Kowloon, Hong Kong, China.
E-mail: yuwang@cityu.edu.hk

Abstract: In engineering practice, soil liquefaction potential is usually evaluated following the cone penetration test (CPT)-based simplified liquefaction triggering procedure. It is widely accepted that CPT-based liquefaction triggering correlation developed from the limited case histories database contains significant model uncertainty. In addition, characterization of spatial distribution of potentially liquefied soils is critical for liquefaction risk assessment and mitigation. However, soil liquefaction potential at untested locations interpolated from limited CPT measurements may involveconsiderable interpolation uncertainty. On the other hand, soil spatial variability can greatly affect the consequences of liquefaction. Neglecting these uncertainties and soil spatial variability may lead to unreliable or even biased liquefaction assessment results. To tackle this challenge, this paper presents a CPT-based probabilistic liquefaction assessment method in a vertical cross-section, which is able to simultaneously consider above-mentioned uncertainties and soil spatial variability. The presented method is demonstrated and validated using real CPT data from Wildlife Liquefaction Array (WLA), USA. The illustration example indicates that the presented method can properly characterize the spatially distributed soil liquefaction potential and estimate the probability of liquefaction at each point within a cross-section.

Keywords: Liquefaction potential; Uncertainty; Spatial variability; Compressive sampling

1 Introduction

In engineering practice, cone penetration test (CPT)-based simplified liquefaction triggering procedure is widely used to evaluate soil liquefaction potential(e.g., Idriss and Boulanger 2008). It is widely acknowledged that liquefaction evaluation results interpreted from limited CPT soundings contain a great deal of uncertainty (e.g., Christian and Baecher 2016). For example, CPT-based liquefaction triggering correlations are usually developed based on the limited case histories database, and thus they involve considerable model uncertainty (e.g., Boulanger and Idriss 2016). Observations from recent earthquakes indicate that spatial variation of soil liquefaction has significant effects on liquefaction-induced damages (e.g., Cubrinovski et al. 2011). However, soil liquefaction is usually evaluated at limited CPT locations, and the spatial distribution of soil liquefaction needs to be interpolated from sparse measurements, leading to interpolation uncertainty in liquefaction evaluation results (e.g., Guan and Wang 2020; Guan et al. 2020). In addition, spatial variability of soil properties may greatly affect liquefaction consequences (e.g., Guan et al. 2021). These lead to an important question in liquefaction assessment: How to probabilistically characterize the spatial distribution of soil liquefaction potential for a given earthquake scenario with proper consideration of liquefaction triggering model uncertainty, interpolation uncertainty and soil spatial variability.

During the past two decades, several CPT-based probabilistic liquefaction assessment methods have been developed (e.g., Juang et al. 2002;Moss et al. 2006). Recently, Idriss and Boulanger (2016) evaluated updated liquefaction case histories database and developed a CPT-based probabilistic liquefaction triggering model. Despite these studies, it is still a challenging task to simultaneously consider above-mentioned uncertainties and soil spatial variability in liquefaction assessment. To tackle this challenge, this paper presents a CPT-based probabilistic liquefaction assessment method in a vertical cross-section based on the work by Guan and Wang (2022). The presented method is illustrated using real CPT data from Wildlife Liquefaction Array (WLA), USA.

2 CPT-based probabilistic liquefaction assessment method

The presented method leverages on anon-Gaussian non-stationary random field generator which combines Bayesian compressive sampling/sensing (BCS) and Markov Chain Monte Carlo (MCMC) simulation. BCS-MCMC random field generator can directly uses limited measured soil properties as input to generate many random field samples of soil properties cross-section with high spatial resolution as output, without the need of pre-determining the types of trend function or auto-correlation function (e.g., Zhao and Wang 2020). CPT-based liquefaction triggering model uncertainty is considered using a Gaussian error term, ε proposed by Idriss and Boulanger (2016). Interpolation uncertainty and soil spatial variability are considered based on the random fields of soil liquefaction resistance. To simultaneously consider the above-mentioned uncertainties and soil spatial variability in liquefaction assessment, Monte Carlo simulation (MCS) is used to repeatedly draw random samples of ε from its prescribed probability distributions and random field samples of soil liquefaction resistance rom limited measurements, which leads to probabilistic liquefaction assessment results. In the presented method, soil liquefaction potential is evaluated following the simplified liquefaction triggering procedure, in which soil liquefaction resistance is quantified in terms of cyclic resistance ratio, CRR, and earthquake loading is expressed in terms of cyclic stress ratio, CSR (e.g., Seed and Idriss 1971). The liquefaction potential of soils is quantified in terms of factor of safety, FS against liquefaction, which is a ratio of CRR to CSR, i.e., FS = CRR/CSR.Fig.1 illustrates the presented probabilistic liquefaction assessment framework, which consists of 10 steps.

Step 1: Compute the corrected equivalent clean sand CPT tip resistance, q_{c1Ncs} for each set of CPT measurements.

↓

Step 2: Generate a random sample of error term, ε in Eq. (4).

↓

Step 3: Estimate cyclic resistance ratio, CRR for each measured q_{c1Ncs} data using the generated sample of ε and Eq. (4).

↓

Step 4: Generate a CRR random field sample from limited CRR data points using Bayesian compressive sensing (BCS) and Markov Chain Monte Carlo (MCMC) simulation.

↓

Step 5: Calculate earthquake loading in terms of cyclic stress ratio, CSR for a given earthquake scenario.

↓

Step 6: Calculate the factor of safety, FS, against liquefaction within the cross-section using the generated CRR random field sample and estimated CSR.

↓

Step 7: Repeat Step 4 to Step 6 many times (e.g., 100 times).

↓

Step 8: Repeat Step 2 to Step 7 many times (e.g., 100 times).

↓

Step 9: Perform statistical analysis for many (e.g., N_B = 100 × 100 = 10,000) generated FS cross-sections.

↓

Step 10: Obtain the spatial distribution of liquefaction probability within the cross-section.

Figure 1. Framework of the presented probabilistic liquefaction assessment method

In Step 1, CPT measurement data including cone tip penetration resistance, q_c and sleeve friction, f_s are collected from each CPT sounding. Then, the corrected equivalent clean sand tip resistance, q_{c1Ncs} is calculated for each set of q_c and f_s using the following equations (e.g., Idriss and Boulanger 2016):

$$q_{c1Ncs} = q_{c1N} + \Delta q_{c1N} \tag{1}$$

$$\Delta q_{c1N} = (11.9 + \frac{q_{c1N}}{14.6})\exp\left[1.63 - \frac{9.7}{\mathrm{FC}+2} - (\frac{15.7}{\mathrm{FC}+2})^2\right] \tag{2}$$

where $q_{c1N} = C_N(q_c / p_a)$ represents tip resistance corrected for overburden stress; overburden correction factor, C_N is expressed as:

$$C_N = \left(\frac{p_a}{\sigma'_v}\right)^{1.338-0.249(q_{c1Ncs})^{0.264}} \leq 1.7 \tag{3}$$

where p_a = 1 atm = 100 kPa; σ'_v = effective overburden stress; Based on regional or local-specific relationships, fines content (FC) may be estimated from the soil behavior type index, I_c which is calculated using CPT q_c and f_s data (e.g., Idriss and Boulanger 2016).

In this study, liquefaction triggering model uncertainty is considered based on a probabilistic model proposed by Idriss and Boulanger (2016):

$$\mathrm{CRR}_{M_w=7.5,\sigma'_v=1\text{ atm}} = \exp\left(\frac{q_{c1Ncs}}{113} + \left(\frac{q_{c1Ncs}}{1000}\right)^2 - \left(\frac{q_{c1Ncs}}{140}\right)^3 + \left(\frac{q_{c1Ncs}}{137}\right)^4 - 2.6 + \varepsilon\right) \tag{4}$$

where ε is a Gaussian random variable with zero mean and a standard deviation of 0.2. $\mathrm{CRR}_{M_w=7.5,\sigma'_v=1\text{ atm}}$ represents the cyclic resistance ratio of soils at earthquake magnitude, M_w = 7.5 and $\sigma'_v = 1$ atm. In Step 2, a random sample of ε is generated from the normal distribution with zero mean and a standard deviation of 0.2. In Step 3, using Eq. (4) and the generated ε sample, CRR of soils for a given earthquake scenario can be calculated as (e.g., Idriss and Boulanger 2016):

$$\mathrm{CRR} = \mathrm{CRR}_{M_w=7.5,\sigma'_v=1\text{ atm}} \times MSF \times K_\sigma \tag{5}$$

Magnitude scaling factor, *MSF* and overburden correction factor, K_σ are expressed as:

$$MSF = 1 + (MSF_{\max} - 1)\left[8.64\exp(\frac{-M_w}{4}) - 1.325\right] \tag{6}$$

$$MSF_{\max} = 1.09 + \left(\frac{q_{c1Ncs}}{180}\right)^3 \leq 2.2 \tag{7}$$

$$K_\sigma = 1 - C_\sigma \ln\left(\frac{\sigma'_v}{p_a}\right) \leq 1.1 \tag{8}$$

$$C_\sigma = \frac{1}{37.3 - 8.27(q_{c1Ncs})^{0.264}} \leq 0.3 \tag{9}$$

Using the following equations, CRR of soils can be estimated at locations with CPT measurements. In order to characterize the spatial distribution of CRR within a cross-section, BCS-MCMC random field generator is adopted to generate many CRR random field samples directly from limited measured CRR data points. Note that the generated random field samples of CRR reflect both soil spatial variability and statistical uncertainty induced by interpolation of limited CRR measurements. Detailed information about BCS-MCMC can be referred to Zhao and Wang (2020). In Step 4, a random field sample of CRR cross-section is generated from limited CRR data points using BCS-MCMC. In simplified liquefaction triggering procedure, earthquake loading in terms of cyclic stress ratio, CSR for a given earthquake scenario is calculated as (e.g., Seed and Idriss 1971):

$$\mathrm{CSR} = 0.65\left(\frac{a_{\max}}{g}\right)\left(\frac{\sigma_v}{\sigma'_v}\right)\mathrm{r_d} \tag{10}$$

where g= gravitational acceleration; σ_v = total overburden stress; $a_{\max}$ = peak ground acceleration at surface; r_{d} is a shear stress reduction factor which is a function of depth, z(Idriss 1999):

$$\begin{aligned} r_{\mathrm{d}} &= \exp(\alpha(z) + \beta(z)M_w) \\ \alpha(z) &= -1.012 - 1.126\sin(z/11.73 + 5.133) \\ \beta(z) &= 0.106 + 0.118\sin(z/11.28 + 5.142) \end{aligned} \tag{11}$$

Using Eqs. (10)-(11), CSR at each point of the cross-section can be obtained. In Step 6, FS at each point within the cross-section is calculated using the generated CRR random field sample and estimated CSR.To incorporate interpolation uncertainty and soil spatial variability, CRR random field sample is repeatedly generated for calculating FS cross-section. Therefore, Steps 4-6 are repeated many times (e.g., 100 times) in Step

7. Similarly, to consider the model uncertainty, ε is repeatedly generated from the normal distribution with zero mean and standard deviation of 0.2 for calculating FS cross-section. Thus, Steps 2-7 are repeated many times (e.g., 100 times) in Step 8. In Step 9, statistical analysis is performed for many (e.g., N_B = 100 × 100 = 10,000) generated FS cross-sections, leading to the full probability distribution of FS at each point within the cross-section. Using the obtained probabilistic results, the probability of liquefaction, P_{liq} over the cross-section can be quantified using the following equation:

$$P_{liq}(x_1, z) = \frac{N_{x_1,z}^{liq}}{N_B} \times 100\% \tag{12}$$

where $P_{liq}(x_1, z)$ represents liquefaction probability at a point (x_1, z); $N_{x_1,z}^{liq}$ indicates the number of generated FS smaller than 1 at the point (x_1, z).

3 Illustration example

In this section, the presented probabilistic liquefaction assessment method is applied to Wildlife Liquefaction Array (WLA), USA during the 1987 Superstition Hills earthquake with M_w = 6.6 and a_{max} = 0.21g. Site investigation results indicate that the site mainly consists of a 3m-3.5m thick non-liquefiable silty clay layer at the ground surface, which is underlain by a 3.5mthick granular soil layer with a saturated unit weight of γ_{sat} = 18kN/m^3 (e.g., Holzer and Youd 2007). The granular soil layer may be liquefied during the Superstition Hills earthquake. The groundwater table is at a depth of 1.2m. Fig. 2illustrates a typical cross-sectionA1-A2 of this site by a solid line. Cross-section A1-A2 has a length of 43m and a depth of 3.5m to 7.0m.Five CPT soundings including CPT-1Cg, CPT-3Cg, CPT-4Cg, CPT-5Cg, and CPT-7Cg were performed within this cross-section, as shown in Fig. 2 by solid triangles.

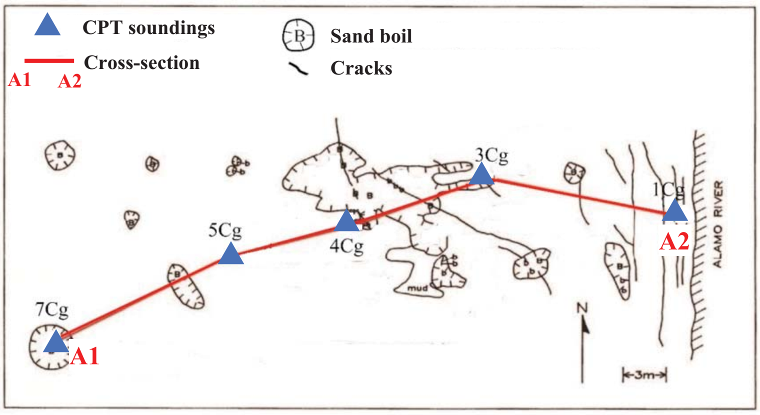

Figure2. Layout of five CPT soundings at the Wildlife Liquefaction Array (after Holzer and Youd 2007)

In Step 1, CPT measurement data including q_c and f_s are collected from each CPT sounding, which are obtained directly from NEES@UCSB website at http: //www.nees.ucsb.edu (accessed March8, 2022). Then, the corrected equivalent clean sand tip resistance, q_{c1Ncs} is calculated using the Eqs. (1)-(3). Fig. 3 shows the calculated q_{c1Ncs} for each CPT sounding. In Steps 2-4, a CRR random field sample is simulated for a given generated ε using BCS-MCMC generator. In Step 5, CSR within the cross-section A1-A2 is calculated using Eqs. (10)-(11) for a_{max} = 0.21g, as illustrated in Fig. 4. In Step 6, FS within the cross-section can be obtained for a given CRR random field sample and estimated CSR. To incorporate model uncertainty, interpolation uncertainty and soil spatial variability, in Steps 7-8, many random samples of ε and CRR cross-section are repeatedly generated to produce many FS cross-sections. In this study, N_B = 10,000 FS cross-sections are generated. The mean and coefficient of variation (COV) of generated FS cross-sections are shown in Fig. 5, respectively.

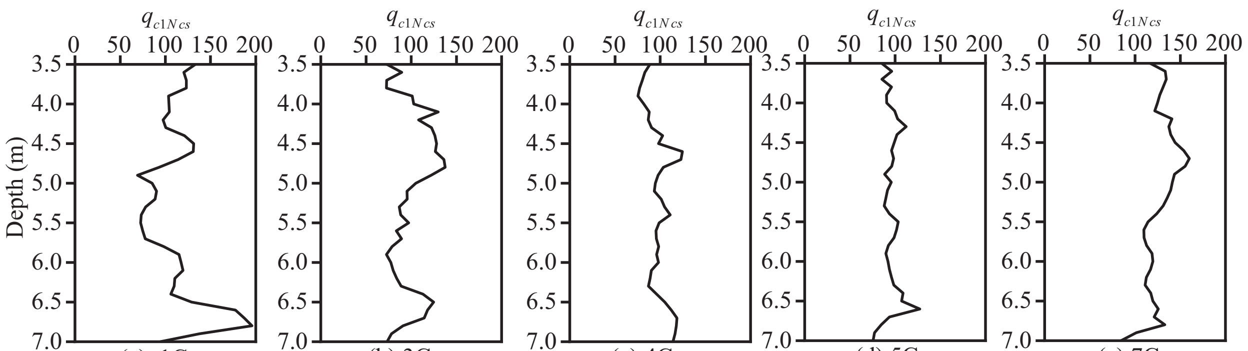

(a) 1Cg (b) 3Cg (c) 4Cg (d) 5Cg (e) 7Cg

Figure 3. Estimated corrected equivalent clean sand tip resistance, $(q_{c1N})_{cs}$ for each CPT sounding

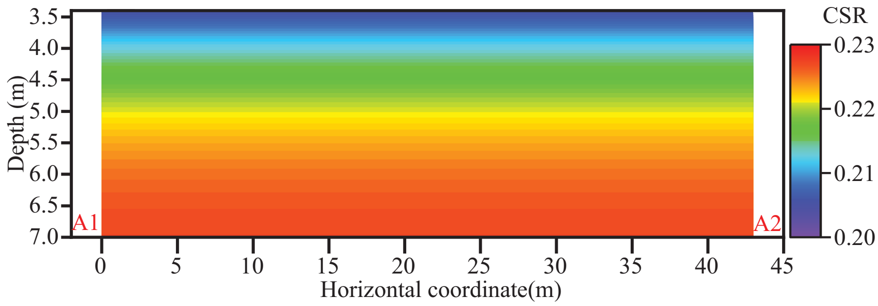

Figure 4. Estimated cyclic stress ratio, CSR in cross-section A1-A2

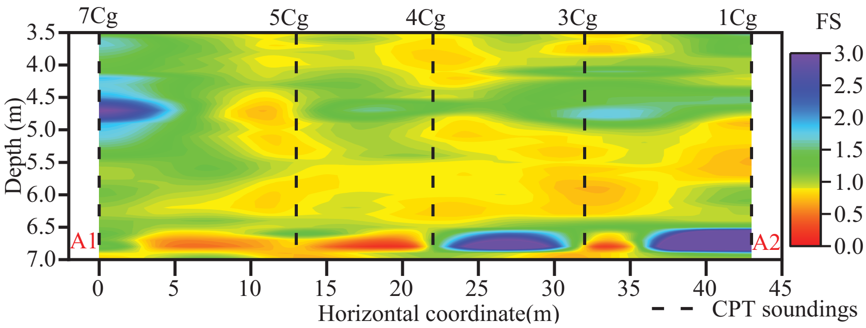

(a) Mean of 10,000 generated FS samples

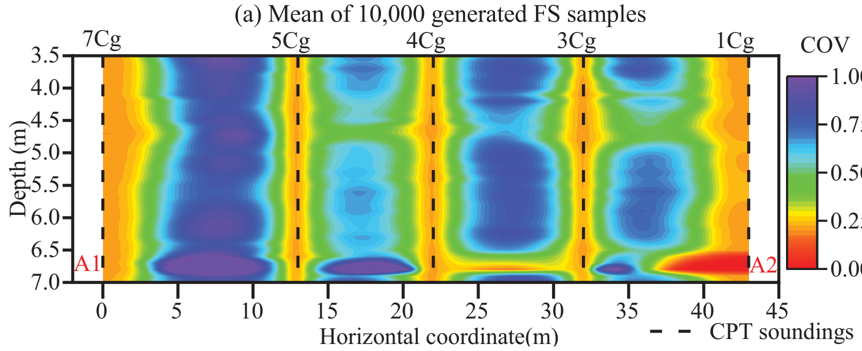

(b) Coefficient of variation (COV) of 10,000 generated FS samples

Figure 5. Cross-section of factor of safety, FS, against liquefaction generated from five CPT soundings

Using Eq. (12), the liquefaction probability at each point of cross-section A1-A2 can be estimated, as shown in Fig. 6. It is found from Fig. 6 that the liquefaction probability of most points within the cross-section is larger than 50%, which indicates that a substantial portion of the granular soil layer is expected to be liquefied within this cross-section during the earthquake. Such liquefaction assessment results are consistent with the site observations during the Superstition Hills earthquake. As reported by Holzer and Youd (2007), widespread sand boils and ground crack were observed at this site, as shown in Fig. 2.

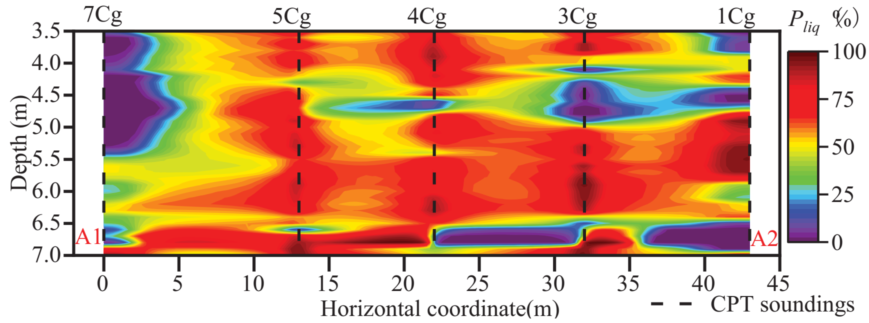

Figure 6. Liquefaction probability, P_{liq}, in cross-section A1-A2

4 Conclusion

This paper presented a CPT-based probabilistic liquefaction assessment method, which is able to simultaneously consider liquefaction triggering model uncertainty, interpolation uncertainty and spatial variability of soil properties. Liquefaction triggering model uncertainty was considered based on the probabilistic model proposed by Idriss and Boulanger (2016). Random field samples of CRR were generated using BCS-MCMC to account for interpolation uncertainty and soil spatial variability. The presented method was demonstrated using real CPT data from Wildlife Liquefaction Array (WLA), USA. The illustration example indicated that the presented method can properly characterize the spatially distributed soil liquefaction potential and quantify the probability of liquefaction at each point within a cross-section.

Acknowledgments

The work described in this paper was supported by a grant from the Research Grant Council of Hong Kong Special Administrative Region (Project No: CityU 11203322), a grant from The Science and Technology Development Fund, Macau Special Administrative Region (File/Project No: SKL-IOTSC(UM)-2021-2023), and a grant from Shenzhen Science and Technology Innovation Commission (Shenzhen-Hong Kong-Macau Science and Technology Project (Category C) No: SGDX20210823104002020), China. The financial support is gratefully acknowledged.

References

Boulanger, R. W., and Idriss, I. M. (2016). CPT-based liquefaction triggering procedure. *Journal of Geotechnical and Geoenvironmental Engineering*, 142(2), 04015065.

Christian, J. T., and Baecher, G. B. (2016). Sources of uncertainty in liquefaction triggering procedures. *Georisk: Assessment and Management of Risk for Engineered Systems and Geohazards*, 10(4), 242-250.

Cubrinovski, M., Bray, J. D., Taylor, M., Giorgini, S., Bradley, B., Wotherspoon, L., and Zupan, J. (2011). Soil liquefaction effects in the central business district during the February 2011 Christchurch earthquake. *Seismological Research Letters*, 82(6), 893-904.

Guan, Z. and Wang, Y. (2020). Statistical charts for determining sample size at various levels of accuracy and confidence in geotechnical site investigation.*Geotechnique*, 70(12), 1145-1159.

Guan, Z. and Wang, Y. (2022). CPT-based probabilistic liquefaction assessment considering soil spatial variability, interpolation uncertainty and model uncertainty. *Computers and Geotechnics*, 141, 104504.

Guan, Z., Wang, Y., and Zhao, T. (2021). Delineating the spatial distribution of soil liquefaction potential in a cross-section from limited cone penetration tests. *Soil Dynamics and Earthquake Engineering*, 145, 106710.

Guan, Z., Wang, Y., Cao, Z., and Hong, Y. (2020). Smart sampling strategy for investigating spatial distribution of subsurface shallow gas pressure in Hangzhou Bay area of China. *Engineering Geology*, 274,105711.

Holzer, T. L., and Youd, T. L. (2007). Liquefaction, ground oscillation, and soil deformation at the Wildlife Array, California. *Bulletin of the Seismological society of America*, 97(3), 961-976.

Idriss, I. M. (1999). An update to the Seed-Idriss simplified procedure for evaluating liquefaction potential. *Proceeding TRB Workshop on New Approaches to Liquefaction*, Publication No. FHWA-RD-99-165, Federal Highway Administration.

Idriss, I. M., and Boulanger, R. W. (2008). Soil liquefaction during earthquakes. Monograph MNO-12, *Earthquake Engineering Research Institute, Berkeley, CA*.

Juang, C. H., Jiang, T., and Andrus, R. D. (2002). Assessing probability-based methods for liquefaction potential evaluation. *Journal of Geotechnical and Geoenvironmental Engineering*, 128(7), 580-589.

Moss, R. E., Seed, R. B., Kayen, R. E., Stewart, J. P., Der Kiureghian, A., and Cetin, K. O. (2006). CPT-based probabilistic and deterministic assessment of in situ seismic soil liquefaction potential. *Journal of Geotechnical and Geoenvironmental Engineering*, 132(8), 1032-1051.

Seed, H. B., and Idriss, I. M. (1971). Simplified procedure for evaluating soil liquefaction potential. *Journal of the Soil Mechanics and Foundations division*, 97(9), 1249-1273.

Zhao, T., andWang, Y. 2020. Non-parametric simulation of non-stationary non-Gaussian 3D random field samples directly from sparse measurements using signal decomposition and Markov Chain Monte Carlo. *Reliability Engineering and System Safety*, 203, 107087.